A UNIVERSAL GAS INTERFACE FOR SIMULTANEOUS ¹⁴C AND δ¹³C MEASUREMENTS

Melina Wertnik[1,2]* • Lukas Wacker[2] • Stefano M. Bernasconi[1] •
Negar Haghipour[1] • Timothy I Eglinton[1] • Caroline Welte[1,2]

[1]Geological Institute, ETH Zürich, Switzerland
[2]Laboratory for Ion-Beam-Physics, ETH Zürich, Switzerland

ABSTRACT. While simultaneous radiocarbon and δ¹³C measurements have been available for organic materials (by accelerator mass spectrometry, AMS, and isotope ratio mass spectrometry, IRMS, respectively), this has not been possible for carbonates until now. Using an existing interface for gas ion source AMS measurements, we developed a prototype for a universal gas interface that allows simultaneous measurement of both carbon isotope ratios from potentially any source of CO_2. First results obtained from reference materials (IAEA-C6, OxaII, PhA, IAEA-C1, IAEA-C2, ETH-4) show that for both organic as well as carbonate samples, the precision of radiocarbon measurements in the coupled mode is comparable to routine standalone AMS measurements. For IRMS δ¹³C measurements, the performance for different materials shows more variation with precisions ranging from 0.07‰ to 0.47‰. However, both organic materials and carbonates can achieve precisions as good as 0.13‰. Once fully automated, the method shows potential for filling the gap of simultaneous carbon isotope measurements for non-organic materials.

KEYWORDS: AMS, carbon, isotope analysis, radiocarbon, stable isotopes.

INTRODUCTION

Carbon isotopes are an essential and widely used source of information for a broad range of research fields, including carbon cycle studies (e.g., Spiker 1980; Repasch et al. 2021), paleoclimate investigations (e.g., Rudzka et al. 2011; Li et al. 2021), and forensic sciences (e.g., Alkass et al. 2011). Radiocarbon tracks atmospheric ¹⁴C concentrations and carries information about ages (Arnold and Libby 1949) or residence times (Reddy et al. 2002). Variations in the stable isotopes of carbon, ¹³C and ¹²C, serve as an indicator for the growth conditions of organisms and the source of carbon, e.g., for differentiating between marine vs. terrestrial origin (Stuiver and Polach 1977). Often both isotopes are needed to make sense of the complex processes involved in the studied archives (Arneborg et al. 1999; Rudzka et al. 2011; Lechleitner et al. 2021; Welte et al. 2021).

Individual carbon isotope measurements by accelerator mass spectroscopy (AMS) are well established (Bennett et al. 1977; Middleton 1984; Ramsey and Humm 2000). With the AMS at ETH, either graphite (Synal et al. 2007) or direct gas measurements (Fahrni et al. 2013; Wacker et al. 2013) can be performed. Graphite measurements are precise but typically require sample sizes of 1 mg C, whereas gas measurements can be used for small samples down to a few μg C and require less preparation time, while providing a precision of around 0.5% (Ruff et al. 2010). This is comparable to other MICADAS laboratories (Mollenhauer et al. 2021; Molnár et al. 2021), even if somewhat higher precisions of 0.2% can be achieved with higher sample sizes (Bard et al. 2015).

Stable isotope measurements of carbon are commonly performed by isotope ratio mass spectrometry (IRMS) (Brenna et al. 1997), where pure CO_2 gas is measured within a stream of helium carrier gas. For continuous flow IRMS, measurements of organic materials using an elemental analyzer (EA) (e.g., Werner et al. 1999) and of carbonate materials by acidification

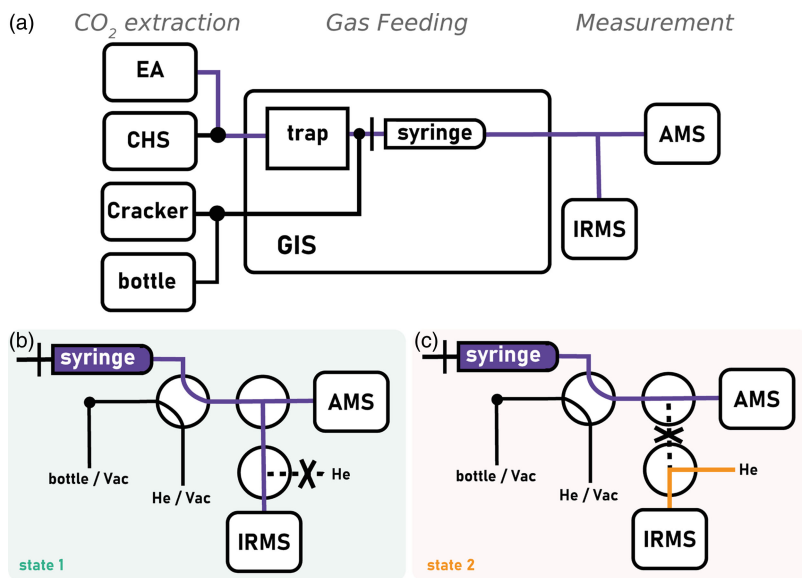*Corresponding author. Email: wertnikm@phys.ethz.ch

Figure 1   (a) Setup schematics. Note that both EA and CHS are connected to the trap, while the Cracker system is directly connected to the syringe. (b) GIS state 1: simultaneous measurement. (c) GIS state 2: AMS only measurement.

with phosphoric acid (e.g., Révész and Landwehr 2002) are widely used. For standalone continuous-flow IRMS, a precision of around 0.1‰ can be readily achieved (Grassineau 2006; Breitenbach and Bernasconi 2011; Trubač et al. 2019).

While individual measurements are already routine, simultaneous measurements of radiocarbon and stable isotopes have so far only been possible for organic materials (McIntyre et al. 2016).

In this study, a novel method was developed that can simultaneously measure both $^{14}C/^{12}C$ and $^{13}C/^{12}C$ from, in principle, any source of CO_2. To this end, an existing gas interface used for gas ion source AMS measurements was modified and tested for simultaneous measurements on both AMS and IRMS using organic and carbonate materials.

METHODS

Simultaneous measurements were developed by adapting an existing gas interface system (GIS) (Wacker et al. 2013) used for routine standalone AMS measurements. To achieve simultaneous measurements, two sequential prime-purge valves as well as capillaries of appropriate interior diameter were added to control the flow of gas between the two mass spectrometers. Using this adapted interface, each measurement can be divided into three distinct steps: CO_2 extraction, gas feeding, and C isotope-ratio measurement (Figure 1).

CO_2 Extraction

Carbon can be extracted from organic samples, carbonates, and cracker samples in the form of CO_2. At ETH, organic samples are burned in an elemental analyzer (EA, Vario ISOTOPE select, Elementar); carbonates are dissolved in phosphoric acid and the CO_2 is subsequently

Table 1   Nominal values of references used.

Reference material	$F^{14}C$	$\delta^{13}C$ (VPDB) [‰]
IAEA-C6	1.5061±0.0011[a]	–10.45±47[b]
OxaII (oxalic acid, NIST SRM4990C)	1.3407±0.0005[c]	–17.8±0.1[c]
PhA (phthalic anhydride)	Blank	–30.01±0.01[e]
IAEA-C1	Blank	2.42±0.33[a]
IAEA-C2	0.4114±0.0003[a]	–8.25±0.31[a,d]
ETH-4	Blank	–10.20±0.03[d]

[a]IAEA (2014).
[b]IAEA (2014).
[c]Stuiver (1983).
[d]Bernasconi et al. (2018).
[e]Sigma, PN-320064-500g, LN-MKBH1376V, in-house calibration.

extracted by the carbonate autosampler (PAL HTC-xt, CTC Analytics). The cracker system enables measurement from ampoules of CO_2 that has been extracted and purified beforehand.

Sample Combustion with EA

Organic samples are weighed into aluminum, tin or silver boats and transferred to the EA autosampler. During combustion, CO_2 and other gases are liberated from the sample. Through the built-in columns of the EA these other gases are removed and only nitrogen and CO_2 exit the EA. To isolate the CO_2, both gases are delivered in chromatographically separated peaks and only the CO_2 peak is transferred to the gas interface system (GIS, Ionplus). For the EA, the carrier gas flow is 220 mL/min during 15 minutes of sampling time. IRMS standards used for the EA are IAEA-C6 and Phthalic Anhydride, cf. Table 1. For the AMS, oxalic acid II (NIST SRM4990C) is used as standard.

CO2 Extraction from Carbonates with CHS

Carbonate materials are weighed into 4 mL septum-sealed glass vials. To remove the air from each vial, they are flushed for approximately 6 minutes with Helium at a flow rate of 80–100 mL/min. Subsequently, the samples are acidified with 100–200 μL of 80% phosphoric acid and placed on a hotplate at 45°C for at least 2 hours. For sampling, the now-liberated CO_2 in the vials is flushed with helium for 2 minutes at 80 mL/min flow and transferred to the GIS. IRMS standards used for the carbonate system are IAEA-C1 and ETH-4, cf. Table 1. For the AMS, a bottle of CO_2 from combusted oxalic acid II is used as standard.

CO2 from Glass Ampules

Cracker samples are pure CO_2 sealed into glass tubes. To ensure a clean break, they are scored in the middle before measurement. Once cracked, the CO_2 is flushed with helium into the GIS. The standard used for the cracker system is a bottle of CO_2 from combusted oxalic acid II.

Gas Handling/Feeding

Once CO_2 has been extracted from the sample, it is passed to the GIS (Ionplus). The GIS is used for routine ^{14}C measurements at the Laboratory of Ion Beam Physics (ETH Zurich, Switzerland), and for this study, it has been adapted to simultaneously fulfil the needs of both mass spectrometers—the AMS (MICADAS) for ^{14}C, and the IRMS (isoprime precisION), for $\delta^{13}C$ analysis. The GIS is necessary to control the CO_2 concentration, pressure, and flow of the gas

mixture into the respective MS ion sources. Two parts of the GIS are responsible for these functions: a zeolite trap to isolate CO_2 and control the concentration, and a syringe with integrated pressure sensor, which controls the flow of the gas into the ion sources. The zeolite trap is designed for small sample sizes (up to 200 µg C). To recover the CO_2 released from the extraction device (EA, carbonate system), the trap is cooled to approximately 11°C. Once all the CO_2 has been trapped, it is released again by heating the trap to 450°C and is flushed into the syringe with helium as carrier gas.

The pressure of the pure CO_2 in the syringe is adjusted to 50–60 mbar by either venting of sample gas or moving the syringe forward. In a last step, helium is added to the syringe until the desired pressure is reached. This results in a concentration of 3.5%–4% CO_2 in helium and ensures optimal conditions for the AMS ion source (Fahrni et al. 2013).

After the syringe, the gas is split between the two mass spectrometers. A valve (prime-purge type, VICI, valco) allows a permanent gas flow to the AMS but can be closed to the IRMS. Between this first valve and the IRMS, an additional valve (prime-purge type, VICI, valco) is added to switch between gas from the syringe and helium. The combination of these two valves allows switching between two states. In the first state, the sample gas flows from the syringe to both AMS and IRMS. In the second state, the sample gas flows from the syringe to the AMS and helium flows to the IRMS (Figure 1).

The AMS requires a steady flow of 1.5–2.5 µg C per minute (Fahrni et al. 2013), which is reached by a combination of the gas pressure in the syringe and the choice of capillaries connecting the syringe with the ion source. The standard capillary from the GIS to the ion source is a fused silica capillary (1 m × 60 µm i.d.) and an additional capillary (6 cm × 60 µm i.d.) was used to connect the two on-off valves.

For standalone AMS measurements, routine syringe pressures result in a carbon flow of 2.0–2.5 µg C/min. This allows for around 25% of the gas to go to the IRMS, while still measuring in the optimal region of carbon flow for the AMS. For the IRMS on the other hand, the minimal signal intensity for the main isotope beam is 1e-9 A, which is achieved with a carbon flow of around 0.1 µg per minute. We conservatively aimed for at least twice this amount, or around 10% of gas, to go to the IRMS. The chosen combination of two capillaries (21 cm × 25 µm i.d. and 1 m × 60 µm i.d.) splits around 15% of the gas to the IRMS. The capillaries are directly connected to the GC-inlet (closed split) without the use of an external open split as the gas flow is much lower than for GC-IRMS. Internally, the IRMS passes the gas over a Nafion dryer before delivery to the ion source.

Isotope Measurements

The measurement scheme chosen for the AMS consists of 10 minutes of measurement time per target. This yields a good balance between sample throughput and counting statistics.

The measurement scheme for the IRMS consists of two peaks of CO_2 reference gas ($\delta^{13}C$ of −38.5‰) delivered 10 minutes apart, with 5 minutes of sample gas in between. The reference gas ensures that there is control over the stability of the IRMS measurement, and the sample gas is timed such that at least 4 minutes pass before the second reference gas peak arrives to allow the ion source to return to baseline conditions. Figure 2 shows an example measurement. The two flat-topped peaks at around 100 s and 750 s in the IRMS current are the reference gas measurements. The sharp peak spike
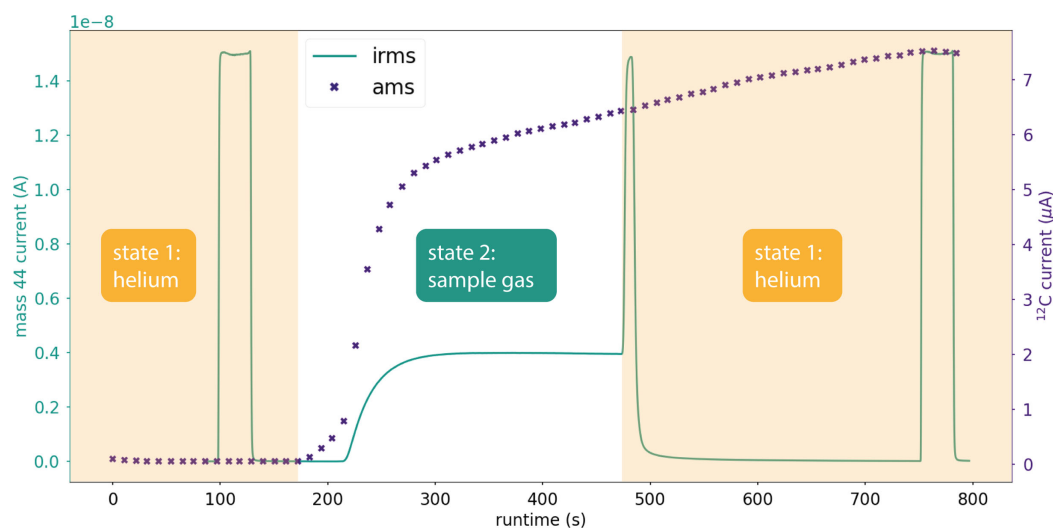
Figure 2   Example of measurement scheme showing both IRMS mass 44 current and AMS ^{12}C current vs. runtime.

around 500 s is caused by switching back to helium which has higher gas flow. The increase in the AMS ^{12}C current is identical to standalone measurements of the same duration.

Measurement of Reference Materials

To demonstrate the novel capabilities of the new method and show a comparison with the existing split method (McIntyre et al. 2016), reference materials for both EA and CHS have been measured. For both methods at least three materials were sought that fulfilled the following criteria: (i) well characterized δ^{13}C values with two that bracket the third for a two-point calibration, (ii) one reference that can be used as a blank reference for the AMS, and (iii) at least one well-characterized material that is not a blank for the AMS. Nominal values for all the materials used in this study are provided in Table 1. All samples were prepared according to the protocol described in the section on CO_2 extraction.

EA:
A batch of 19 references was prepared, with 6x PhA, 6x IAEA-C6, 7x OxaII. Among these, OxaII is used as the standard for the AMS, while IAEA-C6 and PhA are the standards for the IRMS. The AMS blank is also provided by the PhA reference. For each sample 70–850 μg of sample material was weighed into aluminum boats and burnt in the EA for CO_2 extraction.

CHS:
Five batches of carbonate references were prepared for a total of 80 samples (30x IAEA-C1, 30x ETH-4, 20x IAEA-C2). Among these, IAEA-C1 and ETH-4 were used as IRMS standards with the IAEA-C1 providing the AMS blank. For each sample 150–4250 μg of sample material was weighed into 4 mL glass vials for acidification. As previous tests showed that there is some sample size dependence, and the trap of the GIS is built for samples smaller than 200 μg C, standards and samples were weighed in below this threshold. However, to show the effect of sample size, a selection of larger samples above 200 μg C were also prepared (see Discussion).

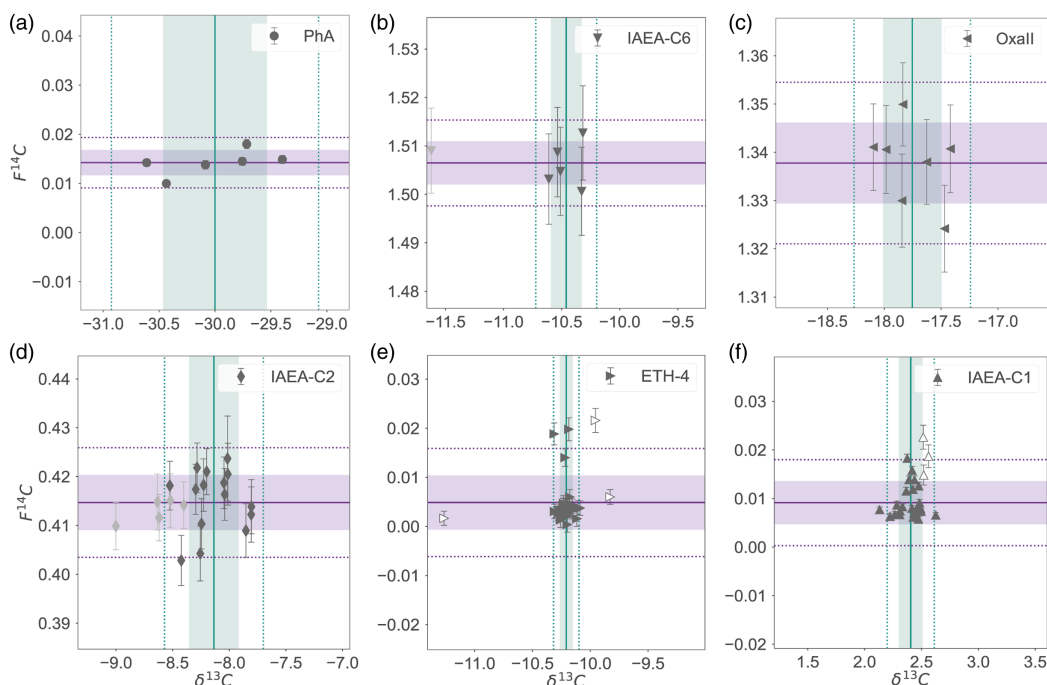Figure 3 (a)–(c) show δ¹³C vs. F¹⁴C of EA measurements and (d)–(f) show δ¹³C vs. F¹⁴C of CHS measurements. The colored band indicates one standard deviation and the dotted lines two standard deviations from mean (solid line). Light gray data points are from samples with masses above 200 μg C and the empty triangles are the outliers described in the main text.

RESULTS

In the following, the results of simultaneous ¹⁴C and ¹³C measurements of different reference materials and for different CO_2 extraction methods are presented.

Results from EA Measurements of Reference Materials

All results are shown in Figure 3 with respective mean values and uncertainties for samples below 200 μg C summarized in Table 2. For why samples above 200 μg C are removed, see the discussion. The measured ¹⁴C values of both IEAE-C6 and the OxaII agree with the nominal values within the uncertainties with relative standard deviations of 0.3% (C6) and 0.6% (OxaII). The blank had a F¹⁴C value of 0.0142±0.0026.

For the ¹³C measurements, the OxaII agrees within uncertainties with the nominal value with a standard deviation of 0.26‰. The standards used to create the two-point calibration had a standard deviation of 0.46‰ (PhA) and 0.13 (IAEA-C6) respectively. While the ¹³C/¹²C in the AMS is used to correct for fractionation, and thus only used as a machine parameter, the mean values for this batch also agree with the nominal values with standard deviations between 0.522‰ and 1.11‰.

Results from CHS Measurements of Reference Materials

Measurements on the CHS were performed over five days. For three samples, no proper measurement was obtained. First, one C1 (122200.25.1) because the cap deformed on the hot

Table 2   Results EA (bold, 1 day) and CHS (5 days). Materials used as IRMS standards are marked with*.

Material	n	Mass range (μg C)	$\delta^{13}C$ (‰ ± σ)	$\delta^{13}C$ AMS (‰ ± σ)	^{14}C measured (F^{14}C ± σ)	Mean error (F^{14}C)
PhA	**6**	**44–198**	**–30.00±0.46***	**–29.70±1.11**	**0.0142±0.0026**[b]	**0.0008**
IAEA-C6	**5**[a]	**80–148**	**–10.46±0.13***	**–10.52±0.522**	**1.5059±0.0047**	**0.0092**
OxaII	**7**	**20–161**	**–17.75±0.26**	**–17.80±0.64**	**1.3378±0.0084**	**0.0090**
IAEA-C1	28/25[c]	54–154	*2.42±0.11**	1.69±2.04	0.0091±0.0033[b]	0.0007
ETH-4	28/27[c]	89–138	*–10.20±0.07**	–10.97±2.37	0.0049±0.0048	0.0016
IAEA-C2	15[a]	18–176	–8.14±0.22	–9.71±1.85	0.4147±0.0056	0.0055

[a]Samples above 200 μg C removed.
[b]Used for blank correction.
[c]F^{14}C measurements include fewer samples (water trap).

plate and the sample gas was lost. Secondly, two ETH-4 (122331.1.13, 122331.1.14) because the fore-vacuum (rough) pump of the IRMS failed during measurement and had to be replaced. For an additional four samples, the water trap of the CHS failed (122200.31.1, 122200.32.1, 122200.33.1, 122331.1.19). For these samples, only the ^{13}C measurements are included as the IRMS has a dedicated Nafion dryer, whereas the MICADAS relies only on the water trap in the CHS. All other samples could be measured, and the results are shown in Figure 3 with respective mean values and uncertainties summarized in Table 2.

The measured ^{14}C concentration of IAEA-C2 agrees with the nominal value within uncertainties, with a relative standard deviation of 1.4%. The F^{14}C value of the blank was 0.0091±0.0033.

The measured δ^{13}C value of the IAEA-C2 agrees within uncertainties with the nominal value with a standard deviation of 0.22‰. The standards used to create the two-point calibration had a standard deviation of 0.11‰ (IAEA-C1) and 0.07 (ETH-4) respectively. The mean values of the δ^{13}C from the AMS agree with the nominal values, but only within large standard deviations between 1.85‰ and 2.04‰.

DISCUSSION

In this section, we compare the precision of our results with that of routine, standalone measurements for the two types of mass spectrometers. For the gas ion source MICADAS at ETH, a precision of 0.5% can be achieved for a modern sample (Fahrni et al. 2013). For continuous flow IRMS methods such as EA-IRMS or CHS-IRMS, precisions around 0.1‰ can be reached routinely (Grassineau 2006; Breitenbach and Bernasconi 2011; Trubač et al. 2019).

EA Measurements

AMS

The ^{14}C blank for the EA measurement day (F^{14}C of 0.0142) was higher than typically observed for conventional blanks at a level of <0.01 F^{14}C (Fahrni et al. 2013). While the subsequent coupled measurement with the CHS had a similar blank level, later coupled CHS measurements showed improved blanks (F^{14}C of 0.0076). Previous tests with the coupled mode from the EA also showed satisfactory blank levels (F^{14}C of 0.009). To constrain what the cause
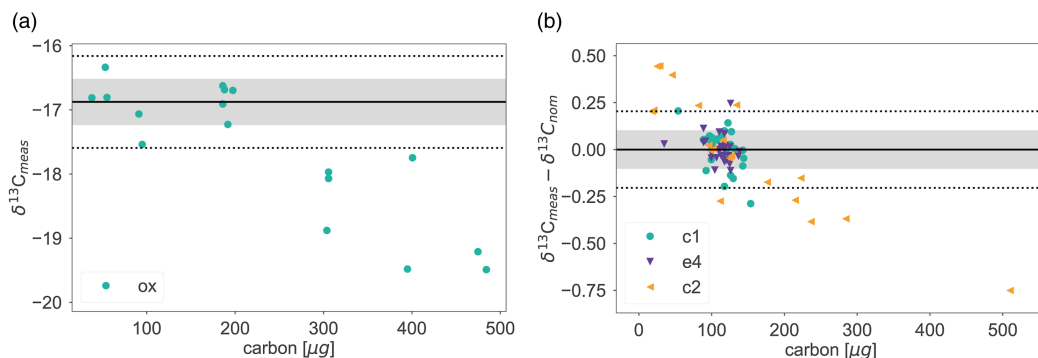
Figure 4 Mass dependence for (a) EA method and (b) CHS method. For both mean and standard deviation have been calculated only for samples between 50 and 200 μg C. Note that for the EA measurement (a) no standards were measured and the δ^{13}C values shown are only relative to the reference gas.

for the elevated blank level on some measurement days is (cross-talk, the batch of acid used, the stripper settings of the AMS, etc.), further investigations are needed.

The precision achieved for the modern samples measured (IAEA-C6, OxaII) was between 0.3‰–0.6‰, which is comparable to routine standalone AMS measurements (0.5‰).

The δ^{13}C uncertainties from the AMS are comparable to standalone AMS measurements, and thus larger than those from the IRMS. As the AMS is not optimized for ^{13}C measurements, but uses the stable isotopes for fractionation correction, this is as expected.

IRMS

While none of the coupled measurements reached the precision of standalone routine measurements (0.1‰), there are large differences in measured scatter between the different reference materials. The PhA had the largest standard deviation of the three materials with 0.46‰. On the other hand, both OxaII and IAEA-C6 were measured much more precisely, suggesting a problem with this particular batch of PhA measurements rather than a general deficiency of the method. Importantly, after removing the IAEA-C6 sample with a size above 200 μg C, the standard deviation of the IAEA-C6 improves to 0.13‰, which shows that it should, in principle, be possible to achieve the desired precision of ∼0.1‰ with further improvements. Removing samples above 200 μg C is reasonable, as the zeolite trap in the GIS was originally designed for small samples up to 200 μg C. By loading larger samples onto the trap, part of the sample is lost leading to isotope fractionation. This effect was previously investigated by measuring OxaII samples of various sizes and is shown in Figure 4. This mass dependence is not seen in the ^{14}C measurements, as any fractionation induced by gas loss is corrected with the ^{13}C measured at the same time, supporting the hypothesis that this is a fractionation effect.

CHS Measurement

AMS

The ^{14}C blank for the CHS measurements (5 days) shows two clusters. The first CHS coupled measurement had an elevated blank, similar to the EA blank (0.0144). The rest of the measurements all had a blank level below the conventional F^{14}C of <0.01, except for the times when the hot plate temperature required adjustment (1 sample) and where the water trap was

not renewed in time (3 samples). This indicates that a satisfactory blank level is achievable with the method provided all components are properly maintained and set.

IAEA-C2 measurements display a precision of 1.4%. This increase in uncertainty compared to a modern sample is in the expected range of material that is half-modern.

While the $\delta^{13}C$ from the AMS agrees with the nominal values within uncertainties, the uncertainties for the CHS measurements are, in general, larger than for the EA batch. From the currently available data it is not clear, whether this stems from the larger number of samples, a difference in the AMS tuning (including the pressure and flow from the GIS) or a general difference between the two methods.

IRMS

For the $\delta^{13}C$ measurements, the precision lies within the uncertainties of the reference materials tested. For both standards a precision better than 0.1‰ was achieved. For the IAEA-C2, we see a similar mass dependence over the mass range of 20–500 µg C as in the EA (Figure 4). By excluding samples above 200 µg C, a reproducibility of 0.22‰ was achieved for IAEA-C2. One reason for the lower precision of this material compared to the two standards might be that it was not homogenized to the same degree, as previously this material was only used for AMS measurements.

However, also the inclusion of samples below 50 µg C seems to increase the standard deviation. With the GIS, the concentration of the gas is independent of sample sizes, and the signal strength in the IRMS is dependent only on the gas pressure and overall carbon flow. Thus, the higher scatter for smaller samples might either be a fractionation effect of the trap, some form of constant contamination from e.g., the acid used, or just a statistical artefact as only 6 samples were below 50 µg C. If the smaller sized samples are isolated, their measured scatter amongst each other is no larger than that of samples around 100 µg C. This could be an indication that it is important to have both samples and standards the same size, but more tests are needed to confirm this.

From all results obtained so far, it therefore seems likely that samples above 200 µg C will consistently suffer from fractionation effects from the trap due to its maximal capacity, whereas smaller sample sizes would need to be investigated further. If keeping to samples around 100 µg C and well homogenized materials, the coupled mode from the CHS achieves precisions comparable to standalone methods.

CONCLUSION

We developed a method for simultaneous ^{14}C and ^{13}C isotopic measurements for carbonates, organic compounds or CO_2 of any source sealed in glass ampoules. In its current state, the method shows promising potential for carbonate measurements with precisions comparable to standalone measurements for both isotopes with sample sizes of 100 µg C. For organic samples, the existing method by McIntyre et al. is still preferred, as it is both more precise and already fully automated. A limitation of the method from this study with the current setup is its dependence on sample sizes. To achieve maximal precision, both samples and standards should be around the same size and below 200 µg C.

Future avenues for improvement of the method include full automation of measurement, optimization of the measurement scheme, further study of small samples and extension to

cracker samples. As the sample gas from cracker tubes doesn't have to pass over the trap, sample sizes are not expected to be as limiting as for other methods. This study also forms the basis for testing more novel CO_2 extraction methods such as laser ablation (LA). Coupling the existing LA setup at ETH (Welte et al. 2016) to the simultaneous measurement method could open up another avenue for measuring carbonate samples.

SUPPLEMENTARY MATERIAL

To view supplementary material for this article, please visit https://doi.org/10.1017/RDC.2023.113

ACKNOWLEDGMENTS

REFERENCES

Alkass K, Buchholz BA, Druid H, Spalding KL. 2011. Analysis of ^{14}C and ^{13}C in teeth provides precise birth dating and clues to geographical origin. Forensic Science International. 209(1–3):34–41. doi: 10.1016/j.forsciint.2010.12.002

Arneborg J, Heinemeier J, Lynnerup N, Nielsen HL, Rud N, Sveinbjörnsdóttir ÁE. 1999. Change of diet of the Greenland Vikings determined from stable carbon isotope analysis and ^{14}C dating of their bones. Radiocarbon 41(2): 157–168. doi: 10.1017/S0033822200019512

Arnold JR, Libby WF. 1949. Age determinations by radiocarbon content: checks with samples of known age. Science 110(2869):678–680.

Bard E, Tuna T, Fagault Y, Bonvalot L, Wacker L, Fahrni S, Synal H-A. 2015. AixMICADAS, the accelerator mass spectrometer dedicated to ^{14}C recently installed in Aix-en-Provence, France. Nuclear Instruments and Methods in Physics Research Section B: Beam Interactions with Materials and Atoms. 361:80–86. doi: 10.1016/j.nimb.2015.01.075.

Bennett CL, Beukens RP, Clover MR, Gove HE, Liebert RB, Litherland AE, Purser KH, Sondheim WE. 1977. Radiocarbon dating using electrostatic accelerators: negative ions provide the key. Science 198(4316):508–510. doi: 10.1126/science.198.4316.508

Bernasconi SM, Müller IA, Bergmann KD, Breitenbach SFM, Fernandez A, Hodell DA, Jaggi M, Meckler AN, Millan I, Ziegler M. 2018. Reducing uncertainties in carbonate clumped isotope analysis through consistent carbonate-based standardization. Geochem Geophys Geosyst 19(9):2895–2914. doi: 10.1029/2017GC007385

Breitenbach SFM, Bernasconi SM. 2011. Carbon and oxygen isotope analysis of small carbonate samples (20 to 100) with a GasBench II preparation device. Rapid Communications in Mass Spectrometry 25(13):1910–1914. doi: 10.1002/rcm.5052

Brenna JT, Corso TN, Tobias HJ, Caimi RJ. 1997. High-precision continuous-flow isotope ratio mass spectrometry. Mass Spectrometry Reviews 16(5):227–258. doi: 10.1002/(sici)1098-2787(1997)16:5<227::aid-mas1>3.0.co;2-j

Fahrni SM, Wacker L, Synal H-A, Szidat S. 2013. Improving a gas ion source for ^{14}C AMS. Nuclear Instruments and Methods in Physics Research B 294:320–327. doi: 10.1016/j.nimb.2012.03.037

Grassineau NV. 2006. High-precision EA-IRMS analysis of S and C isotopes in geological materials. Applied Geochemistry 21(5):756–765. doi: 10.1016/j.apgeochem.2006.02.015

IAEA. 2007. Reference Sheet for Reference Materials IAEA-CH-3 to IAEA-CH-7. https://nucleus.iaea.org/sites/ReferenceMaterials/Shared%20Documents/ReferenceMaterials/StableIsotopes/NBS-22/RS_NBS22_USGS24_IAEA-CH-3-6-7.pdf

IAEA. 2014. Reference Sheet for IAEA-C1 to IAEA-C9 Quality Control Materials, Rev.01. https://nucleus.iaea.org/sites/ReferenceMaterials/Shared%20Documents/ReferenceMaterials/Radionuclides/IAEA-C-1/RS_IAEA-C1_to_IAEA-C9_Rev_01.pdf

Lechleitner FA, Day CC, Kost O, Wilhelm M, Haghipour N, Henderson GM, Stoll HM. 2021. Stalagmite carbon isotopes suggest deglacial increase in soil respiration in western Europe driven by temperature change. Clim Past 17(5):1903–1918. doi: 10.5194/cp-17-1903-2021

Li Y, Yang Yan, Jiang X, Zhao J, Sun Z, Shi X, Tian N, Yang Yunyue, Li J, Duan J. 2021. The transport mechanism of carbon isotopes based on 10 years of cave monitoring: Implications for

paleoclimate reconstruction. Journal of Hydrology. 592:125841. doi: 10.1016/j.jhydrol.2020.125841

McIntyre CP, Wacker L, Haghipour N, Blattmann TM, Fahrni S, Usman M, Eglinton TI, Synal H-A. 2016. Online ^{13}C and ^{14}C gas measurements by EA-IRMS-AMS at ETH Zürich. Radiocarbon. 59(3):893–903. doi: 10.1017/rdc.2016.68

Middleton R. 1984. A versatile high intensity negative ion source. Nuclear Instruments and Methods in Physics Research. 220(1):105–106. doi: 10.1016/0167-5087(84)90416-2

Mollenhauer G, Grotheer H, Gentz T, Bonk E, Hefter J. 2021. Standard operation procedures and performance of the MICADAS radiocarbon laboratory at Alfred Wegener Institute (AWI), Germany. Nuclear Instruments and Methods in Physics Research 496:45–51. doi: 10.1016/j.nimb.2021.03.016

Molnár M, Mészáros M, Janovics R, Major I, Hubay K, Buró B, Varga T, Kertész T, Gergely V, Vas Á, et al. 2021. Gas ion source performance of the EnvironMICADAS at Hekal Laboratory, Deberecen, Hungary. Radiocarbon 63(2):499–511. doi: 10.1017/RDC.2020.109

Ramsey CB, Humm MJ. 2000. On-line combustion of samples for AMS and ion source developments at ORAU. Nuclear Instruments and Methods in Physics Research B 172(1–4):242–246. doi: 10.1016/s0168-583x(00)00116-6

Reddy CM, Pearson A, Xu L, McNichol AP, Benner BA, Wise SA, Klouda GA, Currie LA, Eglinton TI. 2002. Radiocarbon as a tool to apportion the sources of polycyclic aromatic hydrocarbons and black carbon in environmental samples. Environ Sci Technol 36(8):1774–1782. doi: 10.1021/es011343f

Repasch M, Scheingross JS, Hovius N, Lupker M, Wittmann H, Haghipour N, Gröcke DR, Orfeo O, Eglinton TI, Sachse D. 2021. Fluvial organic carbon cycling regulated by sediment transit time and mineral protection. Nat Geosci. 14(11):842–848. doi: 10.1038/s41561-021-00845-7

Révész KM, Landwehr JM. 2002. δ^{13}C and δ^{18}O isotopic composition of CaCO$_3$ measured by continuous flow isotope ratio mass spectrometry: statistical evaluation and verification by application to Devils Hole core DH-11 calcite: Isotopic composition of CaCO$_3$ by CF-IRMS. Rapid Commun Mass Spectrom. 16(22):2102–2114. doi: 10.1002/rcm.833

Rudzka D, McDermott F, Baldini LM, Fleitmann D, Moreno A, Stoll H. 2011. The coupled δ^{13}C-radiocarbon systematics of three Late Glacial/early Holocene speleothems; insights into soil and cave processes at climatic transitions. Geochimica et Cosmochimica Acta 75(15):4321–4339. doi: 10.1016/j.gca.2011.05.022

Ruff M, Fahrni S, Gäggeler HW, Hajdas I, Suter M, Synal H-A, Szidat S, Wacker L. 2010. On-line radiocarbon measurements of small samples using elemental analyzer and MICADAS gas ion source. Radiocarbon 52(4):1645–1656. doi: 10.1017/s003382220005637x

Ruff M, Wacker L, Suter M, Szidat S. 2007. A gas ion source for radiocarbon measurements at 200 kV. Radiocarbon 49. doi:10.2458/azu_js_rc.v.2930

Spiker EC. 1980. The Behavior of ^{14}C and ^{13}C in estuarine water: effects of *in situ* CO$_2$ production and atmospheric exchange. Radiocarbon 22(3):647–654. doi: 10.1017/S0033822200010018

Stuiver M. 1983. International agreements and the use of the new oxalic acid standard. Radiocarbon. 25(2):793–795. doi: 10.1017/S0033822200006159

Stuiver M, Polach HA. 1977. Reporting of ^{14}C data. Radiocarbon 19(3):355–363.

Synal H-A, Stocker M, Suter M. 2007. MICADAS: A new compact radiocarbon AMS system. Nuclear Instruments and Methods in Physics Research B 259(1):7–13. doi: 10.1016/j.nimb.2007.01.138

Trubač J, Magna T, Čejková B, Vondrovicová L, Rapprich V. 2019. Rapid determination of carbon isotope composition in carbonatites using isotope ratio mass spectrometry–comparison of dual-inlet, elemental-analyzer and continuous-flow techniques. Rapid Communications in Mass Spectrometry 33(16):1355–1362. doi: 10.1002/rcm.8482

Wacker L, Fahrni SM, Hajdas I, Molnar M, Synal H-A, Szidat S, Zhang YL. 2013. A versatile gas interface for routine radiocarbon analysis with a gas ion source. Nuclear Instruments and Methods in Physics Research B 294:315–319. doi: 10.1016/j.nimb.2012.02.009

Welte C, Fohlmeister J, Wertnik M, Wacker L, Hattendorf B, Eglinton TI, Spötl C. 2021. Climatic variations during the Holocene inferred from radiocarbon and stable carbon isotopes in speleothems from a high-alpine cave. Clim Past. 17(5):2165–2177. doi: 10.5194/cp-17-2165-2021

Welte C, Wacker L, Hattendorf B, Christl M, Fohlmeister J, Breitenbach SFM, Robinson LF, Andrews AH, Freiwald A, Farmer JR, et al. 2016. Laser ablation–accelerator mass spectrometry: an approach for rapid radiocarbon analyses of carbonate archives at high spatial resolution. Analytical Chemistry 88(17):8570–8576. doi: 10.1021/acs.analchem.6b01659

Werner RA, Bruch BA, Brand WA. 1999. ConFlo III–an interface for high precision δ^{13}C and δ^{15}N analysis with an extended dynamic range. Rapid Commun Mass Spectrom. 13(13):1237–1241. doi: 10.1002/(SICI)1097-0231(19990715)13:13<1237::AID-RCM633>3.0.CO;2-C